Journal of Applied Physics ARTICLE scitation.org/journal/jap

# Magnetization mechanism of a hybrid high temperature superconducting trapped field magnet

Cite as: J. Appl. Phys. **133**, 023902 (2023); doi: 10.1063/5.0133219
Submitted: 2 November 2022 · Accepted: 13 December 2022 ·
Published Online: 9 January 2023



Hengpei Liao,[1] Weijia Yuan,[1] Zhiwei Zhang,[2] and Min Zhang[1,a)]

## AFFILIATIONS

[1]Applied Superconductivity Laboratory, Department of Electronics and Electrical Engineering, University of Strathclyde, Glasgow G1 1XQ, United Kingdom
[2]Department of Electronic and Electrical Engineering, Shanghai Jiaotong University, Shanghai, People's Republic of China

[a)]**Author to whom correspondence should be addressed:** min.zhang@strath.ac.uk

## ABSTRACT

This paper studies the magnetization mechanism of a hybrid high temperature superconducting (HTS) trapped field magnet. To address the size limitation of traditional HTS bulk materials, hybridization between HTS-stacked ring magnets and HTS bulks is proposed here. A jointless HTS-stacked ring magnet is used to increase the trapped field area for HTS bulks. A hybrid HTS magnet with 90 mm in length and 60 mm in width was tested to provide a trapped field of 7.35 T in a field cooling magnetization. The paper focuses mainly on understanding the novel magnetization mechanism of this hybrid HTS trapped field magnet. A numerical model based on homogenized H formulation was used to compare with experimental results, and a good match was found. Our experimental and numerical study of the electromagnetic interaction between the HTS-stacked ring magnet and the HTS bulks reveals that there are two magnetization stages, and the magnetization speed differs in these two stages by a sing criterion: whether the HTS-stacked ring magnet is fully penetrated or not. This study confirms that hybridization helps to build large HTS trapped field magnets.



## I. INTRODUCTION

High temperature superconducting (HTS) bulk materials are widely studied for applications such as magnetic resonance imaging (MRI),[1,2] Maglev,[3] superconducting bearings,[4,5] and superconducting machines.[6–8] Its main advantage is to require a strong magnetic field that cannot be achieved by existing permanent magnets.[3,5] Bulk superconductors based on ReBCO (Re: rare earth) HTS materials have been reported to generate more than 17 T magnetic field by effective magnetization.[9–11] Improvements in magnetization methods have helped to improve the trapped field, e.g., triggering flux jump in pulsed-field magnetization (PFM)[12] and optimizing waveform for the multi-PFM process.[13] However, the intrinsic growing process and low tensile strength of ceramic HTS bulks have led to difficulties in growing homogenized large HTS bulks, which imposes limitations on applications that require larger-size magnets as an alternative solution to HTS bulks.[14]

HTS stack magnets made by cutting and stacking HTS tapes have been studied, and they showed even higher trapped fields than HTS bulks.[15,16] A 17.89 T trapped field by HTS stacks has been demonstrated by field cooling (FC).[17] Again the size of HTS stacks is limited since the maximum width of 2G commercial HTS tapes is 46 mm.[18,19]

On the other hand, HTS-stacked ring trapped field magnets fabricated by commercial HTS coated conductors were proposed due to their flexibility in size.[20–26] The idea of stacking HTS rings was proposed initially by our group in 2017,[23] in which we reported the magnetization and demagnetization properties of the ring magnet at 77 K. The HTS-stacked ring magnets can be made into very large trapped field magnets due to the flexibility in the selection of splitting length. In terms of magnetization study, our group reported a 4.6 T trapped field by field cooling at 25 K in 2020.[26] Pulsed-field magnetization and a thermal controlled persistent current switch (PCS) were employed to investigate the trapped

fields and the magnetization properties of the samples in liquid nitrogen.[24] The downside of the HTS-stacked ring magnet is its low material usage per volume due to its hollow center structure. As a result, the idea of hybridizing two types of HTS trapped field magnets came naturally: adding an HTS-stacked ring magnet can increase the overall magnet size while adding an HTS insert for the HTS-stacked ring magnet can increase the overall material usage per volume. Sheng *et al.* proposed hybridizing round HTS stacks with HTS-stacked ring magnets to increase the overall magnet size and magnetic field strength.[28] Shi *et al.* studied the field distribution of a hybrid ring magnet consisting of a ring-shape magnet and a Bi-2223 hollow tube. It found the declination can be effectively compensated by adjusting the placement of the Bi-2223 tube.[25] All these studies were carried out at 77 K with low fields. So far, there is no study on hybrid HTS trapped field magnets in high magnetic fields. Since the key purpose for a hybrid HTS trapped field magnet is to provide high magnetic field with large sizes for applications, this study is essential. This paper reports a novel hybrid HTS trapped field magnet, aiming at achieving large magnet sizes with a high magnetic field. We focus on hybridizing HTS-stacked ring magnets with HTS bulks, which have not been studied previously. Our hypothesis is that the HTS bulks can effectively improve the total HTS material usage per volume of the HTS-stacked ring magnet while the HTS-stacked ring magnet increases the overall magnet size. We confirmed our hypothesis using a hybrid HTS magnet with 90 mm in length and 60 mm in width. We successfully magnetized the hybrid magnet to 7.35 T using field cooling. This paper will study the magnetization mechanism of the hybrid HTS trapped field magnets using field cooling, in which the electromagnetic interaction between the HTS-stacked ring magnet and HTS bulk becomes interesting. The magnetization mechanism would be related to elucidating the resultant trapped field and improving the design of HTS trapped field magnets, which can realize a higher and larger trapped field for potential applications such as HTS machines.

## II. HTS HYBRID MAGNET PREPARATION

We prepared a hybrid HTS trapped field magnet sample as shown in Fig. 1, by hybridizing an HTS-stacked ring magnet with HTS bulks. Two cylindrical YBCO bulks (OD 16 mm, H 11 mm) from ATZ were inserted into an HTS-stacked ring magnet. The performance of the HTS bulks was tested by FC magnetization at 77 K without any reinforcement process with a 0.8 T field trapped by one HTS bulk. The HTS-stacked ring magnet was formed by two layers of HTS rings with 12 mm Superpower M4 AP tapes. There are 100 HTS rings in one layer, and in total 200 HTS rings as illustrated in Fig 1(a). The critical current of the tapes was 520 A at 77 K. After laser splitting, the critical current is 490 A on average. A hall sensor (Lakeshore HGT-2101) was placed between the two HTS bulks. The hybrid HTS magnet sample was impregnated with wax and aluminum nitride powder. Two aluminum cylindrical bulks were prepared for replacing the HTS bulks for comparison measurements. The finished hybrid magnet has a length of 90 mm and a width of 60 mm, which is restricted by the bore size of the magnetization magnet. In theory, larger hybrid magnets can be made by using HTS rings with longer openings and large HTS bulks.

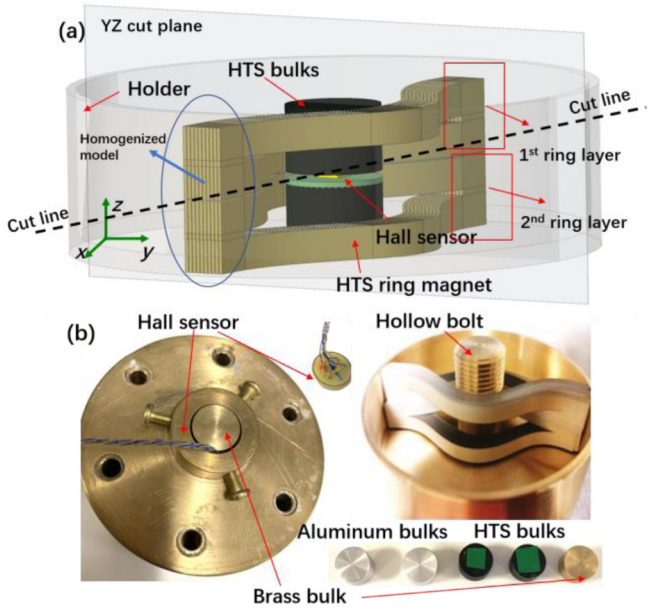


**FIG. 1.** The HTS hybrid trapped field magnet design: (a) scheme of the hybrid magnet design; (b) physical picture of the design. The measurements were carried out with two HTS bulks or two aluminum bulks for comparison.

## III. MEASUREMENT AND RESULTS

The hybrid HTS trapped field magnet was magnetized by a field cooling (FC) magnetization process using the Cambridge Royce Magnet. The sample magnet was cooled down to 25 K in a background field. The magnetic field ramping down rate was 0.075 T/min to minimize the heat generated in the sample. The temperature was controlled by a heater and monitored by a temperature sensor to make sure the magnet temperature stays stable during magnetization. After the measurement of the HTS hybrid magnet, the HTS bulks were then replaced by two aluminum bulks to quantify how the HTS bulks increase the trapped field for the HTS-stacked ring magnet.

In the first magnetization, a 6 T magnetization field was applied and a 5.9 T trapped field was observed for the hybrid magnet, while the stand-alone HTS-stacked ring magnet achieves around 3.5 T under the same magnetization condition as shown in Fig. 2(a). In the second magnetization, the magnetization field was raised to 8 T, and a 7.35 T trapped field for the hybrid magnet was observed, while the stand-alone HTS-stacked ring magnet achieves 3.35 T under the same condition. Figure 2(b) shows the measurement results during the 8 T magnetization. The blue curve indicates the applied field; the red curve indicates the calculated trapped field for the hybrid HTS trapped field magnet, while the green curve indicates the trapped field for the stand-alone HTS-stacked ring magnet. The measurement results showed that the HTS-stacked ring magnet was fully penetrated at 6 T because the stand-alone HTS-stacked ring magnet produced roughly the same amount of trapped field at 6 and 8 T, respectively. This measurement confirms

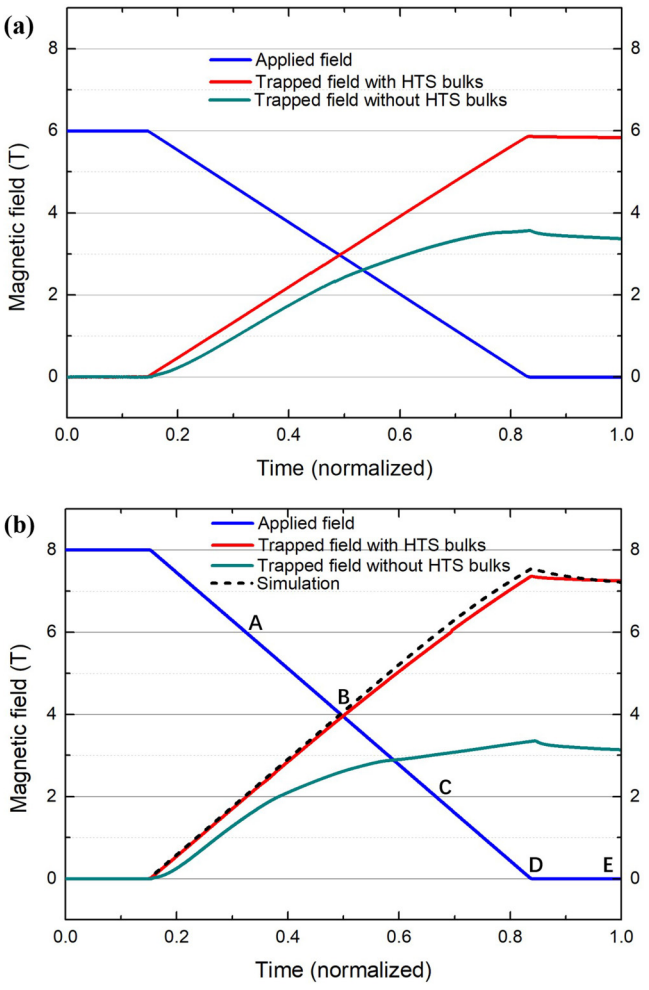


**FIG. 2.** Field cooling magnetization results at 25 K with a 6 T applied field (a) and an 8 T applied field (b).

a record of 7.35 T produced by the HTS hybrid magnet with a length of 90 mm and a width of 60 mm. In our experiment, we used no mechanical reinforcement for HTS bulks because our key focus for hybridizing is not to demonstrate a very high magnetic field to break the existing trapped field record. We use this experiment to prove our hypothesis that hybridizing can create HTS trapped field magnets with large sizes and it can increase the HTS material usage per volume. Our experiment confirmed the hypothesis.

## IV. SIMULATION AND VALIDATION

We are interested in the electromagnetic interaction between the HTS rings and HTS bulks during magnetization. Therefore, a numerical study was carried out to evaluate the current and field distributions of the hybrid magnet during magnetization. We use 3D H formulation to simulate the hybrid HTS trapped field moment, with a governing equation shown in Eq. (1),[27]

$$\mu_0\mu_r\frac{\partial H}{\partial t}+\nabla\times(\rho\nabla\times H)=0, \tag{1}$$

$$\rho=\frac{E_0}{Jcbt}*\left(\frac{J}{J_{cbt}}\right)^{n-1}, \tag{2}$$

where magnetic field intensity $H=[H_x, H_y, H_z]$ are the variables. The relative permeability $\mu_r$ is assumed to be 1 for substrate layers and copper stabilizers which are non-magnetic materials. $\rho$ is the resistivity of HTS materials and is deduced from the E–J power law as shown in Eq. (2).[28] $E_0$ is the critical current criterion equal to 100 $\mu$V/m and $n$ is the power law exponent which is set as 21. Homogenization is used to speed up the calculation, where 10 HTS rings are homogenized into one domain.[26] The field cooling condition is simulated by controlling the applied field with the Dirichlet boundary condition. For the HTS tapes, the magnetic field dependence of critical current density $J_{cbt}$ is considered in the model using direct interpolation of measurements at 25 K. The HTS bulk can trap 0.8 T at 77 K, by which we can get the critical density of the HTS bulk $J_{cbt}$ (0.8 T, 77 K) = $1.7\times10^8$ A/m$^2$ according to Eqs. (3) and (4),[28]

$$B_{trap}=ak\mu_0 J_{cbt}(0.8\,\mathrm{T},\ 77\,\mathrm{K}), \tag{3}$$

$$k=\frac{t}{2a}\ln\left(\frac{a}{t}+\sqrt{1+\left(\frac{a}{t}\right)^2}\right), \tag{4}$$

where $B_{trap}$ is 0.8 T, $a$ and $t$ are the diameter and thickness of the bulk, and $\mu_0$ is vacuum permeability.

The field dependence of $J_{cbt}$ ($B$) at 25 K is calculated with Eq. (5) named Kim model and Eq. (6),[29]

$$J_{cbt}(B)=\frac{J_{cbt}(0)}{\left(1+\frac{|B|}{B_0}\right)}, \tag{5}$$

$$J_{cbt}(T)=J_{cbt}(0)\left(1-\left(\frac{T}{T_c}\right)^2\right)^{1.5}, \tag{6}$$

where $B_0=1.3$ and $T_c=92$ K.

Figure 2(b) shows the trapped field comparison between the 8 T measurement and simulation which agreed well with each other using a normalized time scale. It is worth mentioning that it is not possible to simulate the whole magnetization process on a real time scale (120 min in total). This contributes to the fact that the simulation results are slightly higher than the hall sensor measurements, due to the lack of flux creep in the simulation.

The simulated trapped field profiles for the HTS hybrid magnet and the stand-alone HTS-stacked ring magnet are

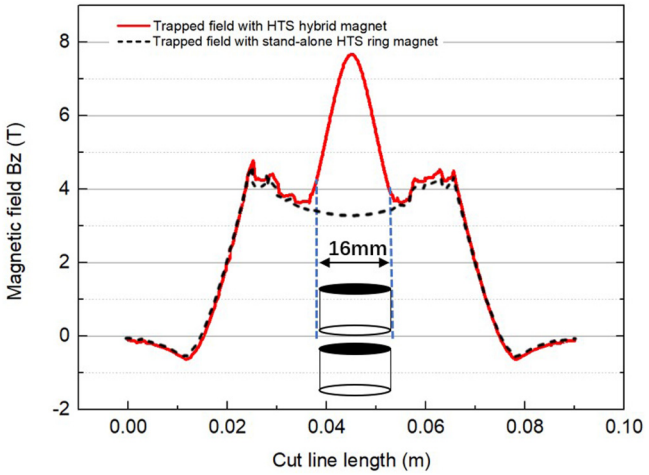


**FIG. 3.** Trapped field distribution along the center cut line of the HTS hybrid magnet and stand-alone HTS-stacked ring magnet.

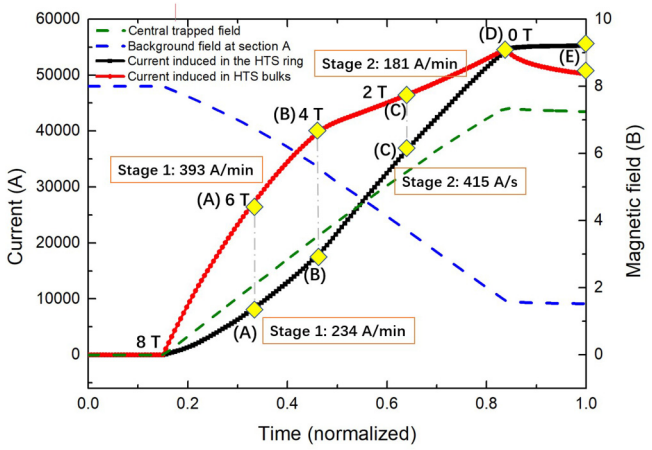


**FIG. 5.** Current increase in the cross sections of the HTS hybrid magnet.

illustrated in Fig. 3. It is clear that the HTS-stacked ring magnet and the HTS bulk both contribute to the 7.35 T trapped field but the trapped field area created by the HTS hybrid magnet is much wider than the stand-alone HTS bulks. The field distribution 2 mm above the HTS hybrid magnet surface is illustrated in Fig. 4. The magnetic flux in this area is calculated by integrating the magnetic flux density and this area, and it achieves 0.005 12 Wb.

## V. MAGNETIZATION MECHANISM

To understand the electromagnetic interaction between the two HTS components, the current distribution in the HTS ring and bulks are calculated during magnetization. Figure 5 shows the total magnetization current generated in the HTS components during the 8 T field cooling: the red line shows the total current induced in the HTS ring (surface integration of section α in Fig. 6) and the black line shows the induced current in the HTS bulk (surface integration of section β in Fig. 6). It is interesting to notice that there is a change of magnetization speed at time B when the applied field is reduced to 4 T. Based on this, we can divide the field cooling magnetization process of this hybrid magnet into two stages. In stage 1 (the applied field changed from 8 to 4 T), the average current increase rate is 393 A/min for the HTS rings and 234 A/min for the HTS bulk. In stage 2 (the applied field changed from 4 to 0 T), the magnetization of the HTS rings slows down, and its current increase rate decreases from 393 to 181 A/min. On the contrary, the magnetization of the HTS bulk speeds up with an increased current increase rate from 234 to 415 A/min on average in stage 2.

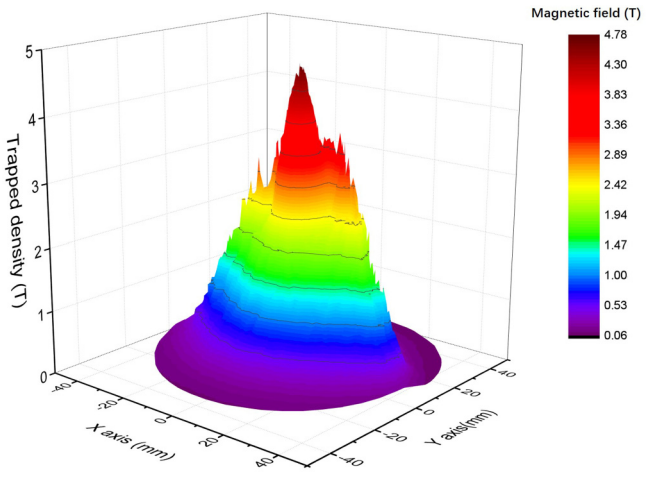


**FIG. 4.** Field distribution at 2 mm above the surface of the HTS hybrid magnet.

Given the applied field is ramping down linearly, the change in the rate of magnetization during the field cooling becomes a question to us. To figure out this question, we simulated the current penetration during the magnetization, and Fig. 6 shows the normalized current distribution in the HTS rings and the HTS bulk for magnetization time steps A, B, C, D, and E, respectively. In time A, both the HTS rings and HTS bulks start to be penetrated, with virgin regions (zero current region) existing in the center of the magnets. The key transition from stage 1 to stage 2 happens at time B, when the HTS rings are fully penetrated (no virgin regions) as shown in the cross-sectional current distribution in Fig. 5. The current penetration of the HTS ring remains the same for time B, C, and D. The only change is the critical current density. From time B on forward, although the magnetization rate of the HTS rings slows down, its induced current is still increasing. To understand this further, we compared two models with a constant critical current density and with a $J_{cbt}$ definition respectively. We notice that the magnetization of the HTS rings model with a constant critical current density stops when it reaches full penetration. However, the HTS rings model with a $J_{cbt}$ definition still sees an increase in the total induced current and trapped field after full penetration, when the applied field keeps ramping down. We,

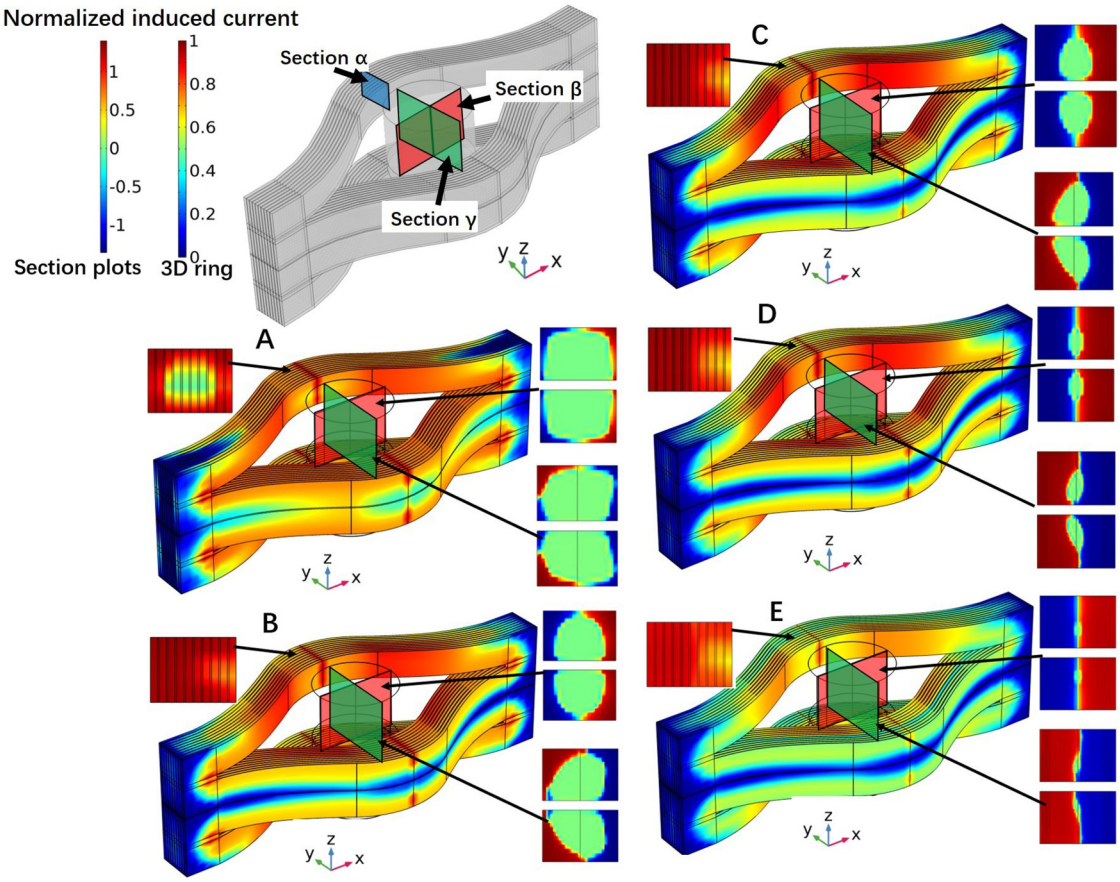


**FIG. 6.** Plots of the spacial current distribution profiles when the applied field is ramped down to 6 (a), 4 (b), 2 (c), 0 T (d), and after flux creep (e).

therefore, conclude that the slowdown of the magnetization for the HTS rings in stage 2 is due to the elimination of the virgin region within the HTS rings. In other words, magnetization slows down when the critical current region is fully penetrated in the HTS ring.

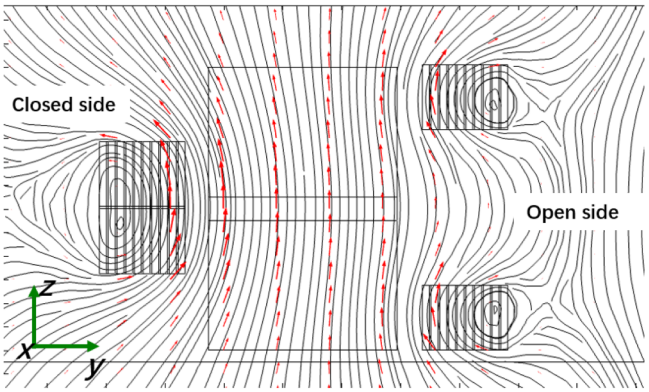


**FIG. 7.** Distribution of magnetic flux generated by HTS-stacked ring magnet.

The slower magnetization is due to the increase of critical current within the HTS rings in stage 2, while the applied field is ramping down (Fig. 5) affecting the $J_{cbt}$ values. The speed-up magnetization of the HTS bulk in stage 2 is to compensate the slowing-down magnetization of the HTS rings. This also suggests that the HTS rings serve as magnetic shielding for the HTS bulks to some extent. The HTS bulks are almost fully penetrated at time E, when flux creep takes place after the field cooling.

A comparison of the HTS bulk current distributions on section β and section γ also unveils an interesting phenomenon that the current penetration is not symmetrical for the HTS bulks. There is both negative and positive current flowing in the left side of the HTS bulk, as shown in time A and time B in Fig. 6. The current distribution in time C and time D also shows the difference between section β and section γ. This can be explained by the asymmetric magnetic field distribution of the HTS-stacked ring magnet. There are lateral magnetic field components generated by the HTS rings, especially at the area near the edges as shown in Fig. 7. The lateral components keep increasing until the HTS rings are fully penetrated at time B, which causes the HTS bulks laterally penetrated in stage 1. To be noted that the HTS bulks used in our

experiments are without reinforcements, both bulks remain integrated under the magnetization processes.

## VI. CONCLUSIONS

This paper proposed a novel hybrid HTS trapped field magnet, consisting of an HTS-stacked ring magnet and an HTS bulk insert. This large hybrid HTS magnet with a length of 90 mm and a width of 60 mm demonstrated a trapped field of 7.35 T in a field cooling magnetization. Interesting electromagnetic interactions between the HTS-stacked ring magnet and the HTS bulk insert are observed during the magnetization. Depending on the induced current increasing rate, we can divide the magnetization into two stages, which are differentiated by whether the HTS-stacked ring magnet is fully penetrated or not. In stage 2, when the HTS-stacked ring magnet is fully penetrated, the HTS-stacked ring magnet will experience a slowing-down magnetization due to the existence of $J_{cbt}$ effects. On the contrary, the HTS bulk will experience a speeding-up magnetization due to the reduction of shielding effects from the HTS-stacked ring magnet. We observe asymmetrical current distribution within the HTS bulks due to the geometrical asymmetry of the HTS-stacked ring magnet. The HTS bulks without reinforcement stayed intact after trapping the 7.35 T field. The proposed hybrid HTS trapped field magnet can potentially create higher magnetic fields with larger magnet sizes, which can be prominent for applications such as HTS machines.

## ACKNOWLEDGMENTS

This research is supported by the Royal Academy of Engineering Research Fellowship for Professor Min Zhang. The authors would like to acknowledge the Henry Royce Institute (Equipment Grant No. EP/P024947/1) for financial support. The authors would like to thank the Cambridge Bulk Group for their technical support during testing.

## AUTHOR DECLARATIONS

### Conflicts of Interest

The authors have no conflicts to disclose.

### Author Contributions

**Hengpei Liao:** Conceptualization (equal); Data curation (equal); Formal analysis (equal); Investigation (equal); Methodology (equal). **Weijia Yuan:** Conceptualization (equal); Data curation (equal); Formal analysis (equal); Funding acquisition (equal); Investigation (equal); Methodology (equal); Project administration (equal). **Zhiwei Zhang:** Data curation (equal); Investigation (equal). **Min Zhang:** Conceptualization (equal); Data curation (equal); Formal analysis (equal); Funding acquisition (equal); Investigation (equal); Methodology (equal); Project administration (equal).

## DATA AVAILABILITY

The data that support the findings of this study are available from the corresponding author upon reasonable request.

## REFERENCES

[1]T. Kii, R. Kinjo, N. Kimura, M. Shibata, M. A. Bakr, Y. W. Choi, M. Omer, K. Yoshida, K. Ishida, T. Komai, K. Shimahashi, T. Sonobe, H. Zen, K. Masuda, and H. Ohgaki, IEEE Trans. Appl. Supercond. **22**, 4100904 (2012).
[2]T. Nakamura, Y. Itoh, M. Yoshikawa, T. Oka, and J. Uzawa, Concepts Magn. Reson., Part B: Magn. Reson. Eng. **31B**, 65 (2007).
[3]Z. Deng, W. Zhang, J. Zheng, B. Wang, Y. Ren, X. Zheng, and J. Zhang, IEEE Trans. Appl. Supercond. **27**, 1 (2017).
[4]J. H. Durrell, M. D. Ainslie, D. Zhou, P. Vanderbemden, T. Bradshaw, S. Speller, M. Filipenko, and D. A. Cardwell, Supercond. Sci. Technol. **31**, 103501 (2018).
[5]F. N. Werfel, U. Floegel-Delor, R. Rothfeld, T. Riedel, B. Goebel, D. Wippich, and P. Schirrmeister, Supercond. Sci. Technol. **25**, 014007 (2012).
[6]D. Zhou, M. Izumi1, M. Miki, B. Felder, T. Ida, and M. Kitano, Supercond. Sci. Technol. **25**, 103001 (2012).
[7]M. Miki, S. Tokura, H. Hayakawa, H. Inami, M. Kitano, H. Matsuzaki, Y. Kimura, I. Ohtani, E. Morita, H. Ogata, M. Izumi, H. Sugimoto, and T. Ida, Supercond. Sci. Technol. **19**, S494–S499 (2006).
[8]Y. Zhang, D. Zhou, T. Ida, M. Miki, and M. Izumi, Supercond. Sci. Technol. **29**, 044005 (2016).
[9]M. Tomita and M. Murakami, Nature **421**, 517–520 (2003).
[10]Y. Shi, D. Namburi, W. Zhao, J. H. Durrell, A. R. Dennis, and D. A. Cardwell, Supercond. Sci. Technol. **29**, 015010 (2016).
[11]J. H. Durrell, A. R. Dennis, J. Jaroszynski, M. D. Ainslie, K. G. B. Palmer, Y. H. Shi, A. M. Campbell, J. Hull, M. Strasik, E. E. Hellstrom, and D. A. Cardwell, Supercond. Sci. Technol. **27**, 082001 (2014).
[12]D. Zhou, M. D. Ainslie, Y. Shi, A. R. Dennis, K. Huang, J. R. Hull, D. A. Cardwell, and J. H. Durrell, Appl. Phys. Lett. **110**, 062601 (2017).
[13]Y. Tsui, D. Moseley, A. R. Dennis, Y. Shi, M. Beck, V. Cientanni, D. Cardwell, J. Durrell, and M. Ainslie, IEEE Trans. Appl. Supercond. **32**, 6800105 (2022).
[14]J. R. Hull and M. Murakami, Proc. IEEE **92**, 1705–1718 (2004).
[15]A. Patel, S. C. Hopkins, and B. A. Glowacki, Supercond. Sci. Technol. **26**, 032001 (2013).
[16]T. Tamegai, T. Hirai, Y. Sun, and S. Pyon, Phys. C **530**, 20–23 (2016).
[17]M. Suyama, S. Pyon, Y. Iijima, S. Awaji, and T. Tamegai, Supercond. Sci. Technol. **35**, 02LT01 (2022).
[18]M. Suyama, S. Pyon, Y. Iijima, S. Awaji, and T. Tamegai, Supercond. Sci. Technol. **34**, 065004 (2021).
[19]A. Patel, A. Baskys, T. M. Williams, A. McCaul, W. Coniglio, J. Hänisch, M. Lao, and B. A. Glowacki, Supercond. Sci. Technol. **31**, 09LT01 (2018).
[20]S. Lee, W. Kim, Y. Kim, S. Park, J. Lee, J. Hahn, G. Hong, H. Park, C. Park, and K. Choi, IEEE Trans. Appl. Supercond. **23**, 4601305 (2013).
[21]G. A. Levina, P. N. Barnes, J. Murphy, L. Brunke, J. D. Long, J. Horwath, and Z. Turgut, Appl. Phys. Lett. **93**, 062504 (2008).
[22]H. G. Lee, J. G. Kim, S. W. Lee, W. S. Kim, S. W. Lee, K. D. Choi, G. W. Hong, T. K. Ko *et al.*, Phys. C **445–448**, 1099–1102 (2006).
[23]J. Sheng, M. Zhang, Y. Wang, X. Li, J. Patel, and W. Yuan, Supercond. Sci. Technol. **30**, 094002 (2017).
[24]J. Sheng, Y. Pan, J. Jiang, W. Li, B. Shen, Z. Zhang, and W. Wu, IEEE Trans. Appl. Supercond. **29**, 1–5 (2019).
[25]J. Shi, X. Li, and J. Sheng, IEEE Trans. Appl. Supercond. **32**, C1 (2022).
[26]M. Z. Ali, J. Zheng, F. Huber, Z. Zhang, W. Yuan, and M. Zhang, Supercond. Sci. Technol. **33**, 04LT01 (2020).
[27]M. Zhang and T. A. Coombs, Supercond. Sci. Technol. **25**, 015009 (2012).
[28]M. D. Ainslie and H. Fujishiro, Supercond. Sci. Technol. **28**, 053002 (2015).
[29]S. Zou, V. M. R. Zermeño, and F. Grilli, IEEE Trans. Appl. Supercond. **26**, 4702405 (2016).